Polar Science 27 (2021) 100597

Contents lists available at ScienceDirect

Polar Science

journal homepage: http://www.elsevier.com/locate/polar

Variation in recent annual snow deposition and seasonality of snow chemistry at the east Greenland ice core project (EGRIP) camp, Greenland

Fumio Nakazawa [a,b,*], Naoko Nagatsuka [a], Motohiro Hirabayashi [a], Kumiko Goto-Azuma [a,b], Jørgen Peder Steffensen [c], Dorthe Dahl-Jensen [c]

[a] National Institute of Polar Research, 10-3 Midori-cho, Tachikawa, Tokyo 190-8518, Japan
[b] The Graduate University for Advanced Studies, SOKENDAI, Shonan Village, Hayama, Kanagawa 240-0193, Japan
[c] Physics of Ice Climate and Earth, Niels Bohr Institute, University of Copenhagen, Tagensvej 16, DK-2200 Copenhagen N, Denmark

ARTICLE INFO

Keywords:
Greenland
Snow
Chemistry
Dust
Accumulation

ABSTRACT

We collected snow samples from two pits with depths of 4.02 and 3.18 m at the East Greenland Ice Core Project camp (75°37′N, 35°59′W), Greenland in the summer of 2016 to estimate recent annual snow deposition and examine seasonal variation in major ion species, stable isotopes of water and microparticles (dust). Dating based on clear seasonal variation in chemical components indicated that the 4.02- and 3.18-m-deep pits included snow deposition corresponding to ten years from 2006 to 2016 and seven years from 2009 to 2016, respectively. The mean values for annual snow deposition for the 4.02-m-deep pit were 138 and 145 mm yr^{-1} in water equivalent (mm w.e. Yr^{-1}) in 2006–2016 and 2009–2016, respectively. The average deposition for the 3.18-m-deep pit was 149 mm w.e. Yr^{-1} between 2009 and 2016. Seasonal variation in concentrations of major ion species and dust were similar to those previously reported for Greenland. The maximum Cl^{-}/Na^{+} concentration ratios in the summer were much higher than the ratios at other sites in Greenland.

1. Introduction

Acceleration in global sea level rise can be linked to mass loss from the Greenland ice sheet due to increases in surface meltwater runoff (Trusel et al., 2018) and ice stream discharge (Van den Broeke et al., 2009). Rapid changes in ice dynamics may accelerate mass loss (Vallelonga et al., 2014). A comprehensive understanding of the mechanisms underlying such changes is important because they are directly linked not only to the global sea level rise but also to changes in ocean circulation and climate.

The North-East Greenland Ice Stream (NEGIS) is the largest ice stream in Greenland and the only ice stream extending inland (Fahnestock et al., 1993, 2001; Joughin et al., 2001). The onset of the streaming flow, likely with a horizontal flow velocity of several tens of meters per year, is at the central ice divide, terminating in three large outlet glaciers approximately 1000 km downstream (Vallelonga et al., 2014).

Reported snow accumulation rates in the area are lower than those in northwestern Greenland (Bigler et al., 2002; Vallelonga et al., 2014). The North Greenland Traverse (NGT) program (Fischer et al., 1998) drilled more than 50 firn and ice cores up to 200 m in northern Greenland in 1993–1995. Rates of accumulation were lower in the eastern area of the Greenland ice divide than in the western area.

Most deep ice core drilling in Greenland has been carried out along the central ice divide due to the slow ice flow (Vallelonga, 2014). No deep ice core has been obtained in northeastern Greenland.

The East Greenland Ice Core Project (EGRIP), an international ice coring project and an initiative of the University of Copenhagen in Denmark, was launched in 2015 as the first deep ice coring project in the area. The EGRIP ice core is expected to advance our knowledge of the dynamics and past changes of the Greenland Ice Sheet as well as past climate change. Japanese scientists are participating in the project as part of the Arctic Challenge for Sustainability (ArCS) project, and cooperative research is underway involving various countries.

As a preliminary study toward the start of an ice core analysis, it is important to understand the factors that affect the chemical components in snow, such as seasonal variation and source, and the characteristics of the depositional environment, such as surface mass balance and melt effects, at the EGRIP site. Here, we present a reconstruction of recent annual snow deposition based on snow pit studies conducted at EGRIP in the 2016 summer season. We also performed a detailed glaciochemical

* Corresponding author. National Institute of Polar Research, 10-3 Midori-cho, Tachikawa, Tokyo, 190-8518, Japan.
E-mail address: nakazawa@nipr.ac.jp (F. Nakazawa).

https://doi.org/10.1016/j.polar.2020.100597
Received 5 February 2020; Received in revised form 23 September 2020; Accepted 24 September 2020
Available online 14 October 2020
1873-9652/

analysis of seasonal variation in major ion species, stable isotopes of water and microparticles (dust), and evaluated sources of chemical species in the snow samples.

2. Study area and methods

From the end of June to the beginning of July 2016, snow pit observations were performed at two sites, Pit 1 and Pit 2 (2666 and 2660 m a.s.l., respectively), on the east side of the EGRIP camp (75°37′N, 35°59′W) in East Greenland (Fig. 1). The direct distance between the two sites was approximately 650 m and Pit 1 was northwest of Pit 2. The depths were 4.02 m for Pit 1 and 3.18 m for Pit 2.

Data for stratigraphy, temperature, and density of snow were recorded. To measure the density, a specially designed square-shaped sampler with a capacity of 100 cm^3 was inserted horizontally into the pit walls. Then, a snow sample was removed and weighed. Sampling was performed at consecutive intervals of 0.03 m.

Additional snow samples were collected for analyses of ion species (Na^+, K^+, NH_4^+, Mg^{2+}, Ca^{2+}, Cl^-, NO_3^-, SO_4^{2-}, and $CH_3SO_3^-$ [hereafter, MSA]), dust (particle size of 0.52–12 μm) and stable isotopes of water ($\delta^{18}O$ and δD). The samples were taken consecutively at intervals of 0.03 m using a plastic spatula and a ceramic knife that were pre-cleared. Each snow sample was placed into a dust-free plastic bag for major ion and stable water isotope analyses or into a pre-cleaned plastic cup (Thermo Scientific Nalgene, Straight-Side Wide-Mouth Jar) for the dust analysis.

The samples for the ion and stable isotope analyses were melted in the bags, transferred to pre-cleaned polypropylene bottles (SCC Iboy, 100 mL; AS ONE Corporation, Osaka, Japan) and refrozen at the EGRIP camp. Samples for the dust analysis were kept frozen. All samples were finally transported to the National Institute of Polar Research in the frozen state.

In the laboratory, the samples were melted again and ions were analyzed in a class 10,000 clean room by ion chromatography (Dionex ICS-5000+; Thermo Fisher Scientific, Waltham, MA). IonPac AS11-HC and CS14 columns were used for anion and cation analyses, respectively. The analytical precision was better than 2% at the 1 ng mL^{-1} level for all ions. In the same clean room, the samples for the dust analysis were transferred to glass beakers and melted prior to analysis. Dust concentrations in the samples were measured in the clean room using a Coulter counter (Multisizer 4; Beckman Coulter Inc., Brea, CA). The error of measured values was approximately 10%. $\delta^{18}O$ and δD were measured using a dual-inlet isotope mass spectrometer (Delta V; Thermo Fisher Scientific) by an equilibrium method in a laboratory next to the clean room. The precision (1σ) was 0.05% for $\delta^{18}O$ and 0.5% for δD (Uemura et al., 2004).

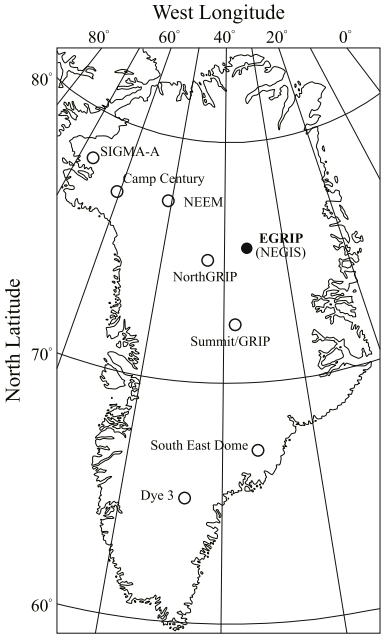

Fig. 1. Location of the study area (black circle) and previous ice core drilling sites (open circle) in Greenland.

3. Results and discussions

3.1. Snow temperatures and stratigraphy in the pits

The snow temperature profiles of the two pits are summarized in Fig. 2; temperatures were below freezing in all layers and decreased from the surface to the bottom of the pits. Owing to the inclement weather and time constraints, temperatures for both pits were measured over two days each. On the second day, digging was resumed from the final depth on the previous day; the temperature of the newly exposed pit wall was measured from 2.00 m for Pit 1 and 2.70 m for Pit 2. The time interval between the measurements was six days for Pit 1 and one night for Pit 2. This increased the snow temperature in the uppermost tens of centimeters. In the lower depths, the trend became consistent with previous temperature readings.

The stratigraphies for the pits indicated three snow types. The dominant snow type was depth hoar. Compacted snow layers on the surfaces and ice layers were also observed (Fig. 3). Ice layers of several millimeters in thickness were detected at depths of 1.76 m and 2.02 m for Pit 1. For Pit 2, ice layers of 1–2 mm in thickness appeared at 1.865 m and 1.875 m. Additionally, thick ice layers of 10–20 mm were observed at depths of 2.030–2.045 m and 2.24–2.26 m. In addition, inhomogeneous (uneven or patchy) ice layers were seen at 2.18–2.19 m and 2.21–2.22 m depths. At 2.00–2.24 m, vertical ice channels, indicating that meltwater passed through the firn and refroze into the layers of the previous year, were observed. These ice layers provide evidence that slight summer surface melting or internal melting in subsurface layers occurred at the EGRIP site. Internal melting of snow is driven by radiative heating, which is produced by absorption of penetrating shortwave solar radiation. However, this melting was not sufficient to disturb the stable water isotope and ion profiles.

3.2. Dating of snow pits

Dating of the snow pits was conducted using the profiles of $\delta^{18}O$, δD, deuterium-excess (= δD – 8$\delta^{18}O$; hereinafter, d-excess), and MSA

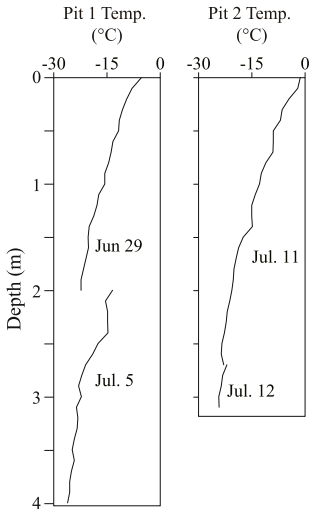

Fig. 2. Vertical profiles of snow temperature for Pit 1 and Pit 2.

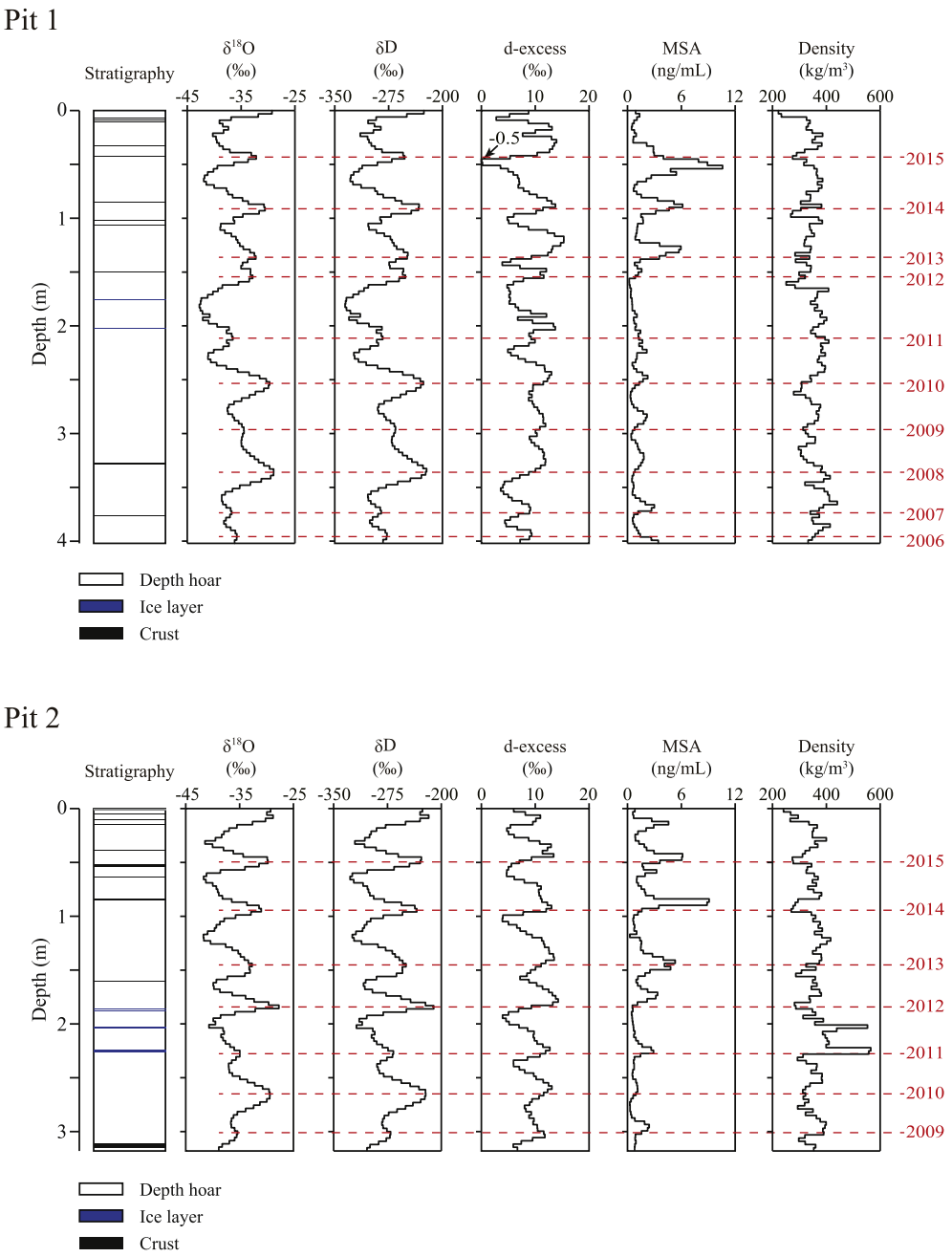

Fig. 3. Vertical profiles from the pit samples at EGRIP. Physical stratigraphy, stable isotopes of water ($\delta^{18}O$ and δD), deuterium-excess value (d-excess), $CH_3SO_3^-$ (MSA) concentration, and snow density are shown. Red dotted lines indicate annual boundaries estimated from peaks of $\delta^{18}O$, δD, d-excess, and MSA. (For interpretation of the references to colour in this figure legend, the reader is referred to the Web version of this article.)

(Fig. 3). We assume that observed cyclic changes in $\delta^{18}O$ and δD are annual cycles. Previous studies of other sites in Greenland have reported a correlation between stable isotopes and temperature (e.g., Steffensen, 1985; Finkel et al., 1986; Beer et al., 1991; Kuramoto et al., 2011). This indicates that $\delta^{18}O$ and δD values have maxima and minima in the summer and winter layers, respectively. In fact, our pit sites exhibited maxima near the snow surface in the summer of 2016 in the $\delta^{18}O$ and δD profiles. Hence, each stable isotope cycle should indicate deposition for a given year, and the dating results are shown in Fig. 3.

The seasonal variation in d-excess supports our dating results and enables the identification of seasonal layers between the summer and autumn. The value of d-excess depends on the sea surface temperature and evaporation processes of sea water in the vapor source region (e.g., Uemura, 2007). At the ice core drilling sites in Greenland, maximum and minimum d-excess values have been observed in the autumn and from spring to early summer, respectively (Johnsen et al., 1989; Kuramoto et al., 2011). Each d-excess maximum in this study appeared above the layer with the annual maxima for $\delta^{18}O$ and δD. This corresponded to peaks in the summer for the stable isotopes and autumn for d-excess. Because the maximum and minimum values for the stable isotopes mark the summer and winter, whereas the d-excess maximum marks autumn, these peaks are markers of both annual and seasonal layers.

We also used seasonal variation in MSA for dating. MSA is regarded as having a single source, namely, marine biogenic activity (e.g., Wendl et al., 2015), while other ions measured in this study have multiple emission sources. Thus, the time-series data for the MSA profile are expected to show that the seasonal variation is only due to variation in marine biogenic activity. In this study, annual maxima of MSA

concentrations were mostly detected above the summer layers identified by the $\delta^{18}O$ and δD profiles. Previous studies of the air and snow at Dye 3, Summit and NEEM in Greenland have reported two peak seasons with respect to MSA concentrations in a year: spring and late summer-autumn (Li et al., 1993; Jaffrezo et al., 1994; Kuramoto et al., 2011). Our pits recorded only late summer-autumn peaks in the MSA profiles. The late summer to autumn peak may be attributed to the oxidation of regional dimethyl sulfide (DMS) emissions after the retreat of sea ice around Greenland, as described by Kuramoto et al. (2011). As explained above, the MSAprofiles in our pits showed clear seasonal variation peaking in late summer-autumn and support the accuracy of our dating.

The ice layers at depths of 1.76 m and 2.02 m for Pit 1 and 2.04 m and 2.25 m for Pit 2 formed in the summer of 2012. These ice layers appeared between the summer 2011 and summer 2012 layers according to our dating (Fig. 3). Surface snow/ice melting was observed over the Greenland Ice Sheet in July 2012 (Nghiem et al., 2012; Tedesco et al., 2013; Aoki et al., 2014). In addition, a remarkable amount of rainfall, estimated to be in the range of 60–100 mm, was observed from 10 July to July 13, 2012 at SIGMA-A (78°03′N, 67°38′W, 1490 m a.s.l., Fig. 1) on the northwestern part of the Greenland ice sheet (Aoki et al., 2014). Therefore, meltwater should also occur at the EGRIP site in the summer of 2012, penetrate lower layers and refreeze in the layer between the summers of 2011 and 2012. The accuracy of our dating could explain this melting phenomenon well.

3.3. Annual snow deposition

As stated above, the snow pits were dated by counting annual maxima in stable isotopes, d-excess and MSA profiles. The numbers of annual cycles indicated that the snow at depths of 4.02 m for Pit 1 and 3.18 m for Pit 2 included deposits corresponding to ten-year period from 2006 to 2016 and seven-year period from 2009 to 2016, respectively. The estimated thicknesses of the pits were 1402 mm and 1121 mm in water equivalent (w.e.) from the density profiles in Fig. 3. The average annual snow deposition was 138 mm w.e. Yr^{-1} in 2006–2016 for Pit 1. For 2009–2016, the average values were 145 mm w.e. Yr^{-1} and 149 mm w.e. Yr^{-1} for Pit 1 and Pit 2, respectively.

Variation in annual snow deposition reconstructed from the two pits appeared to be maintained at approximately 150 mm w.e. Yr^{-1}, except in some years (Fig. 4). The annual snow deposition ranged from 58 to 202 mm w.e. Yr^{-1} for Pit 1 and from 126 to 188 mm w.e. Yr^{-1} in Pit 2.

Although the amounts of annual precipitation should be similar because the two pit sites were close to one another, the extent of fluctuation in annual snow deposition differed between the two pits. This may be explained by the difference in degree of surface unevenness. Snow deposition on a convex surface may be relatively low compared with surrounding areas in the following year, whereas concave surfaces may receive large amounts of snow to maintain a relatively flat surface.

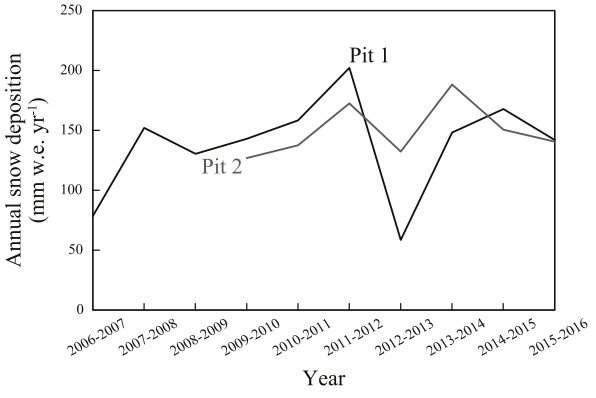

Fig. 4. Reconstructed annual snow depositions for Pit 1 (black line) and Pit 2 (gray line).

As a result, the average values for the two pits were similar.

The reconstructed values for annual deposits in 2011–2012 and 2012–2013 in both pits should be influenced by snow melting events occurring in the summer of 2012. Refrozen ice layers generated by percolation of the snow meltwater in the summer of 2012 were found between the layers corresponding to the summers of 2011 and 2012. This seems to correspond with a reduction in annual snow deposition from the summers of 2012–2013 and an increase between the summers of 2011 and 2012. The heterogeneous distribution of these ice layers may explain the between-site difference in the annual deposition records during that time.

Table 1 shows a summary of average annual deposition for the present day at other deep ice core drilling sites in Greenland. The period covered by each average value was not reported by Steen-Larsen et al. (2011). The average value at NEEM was based on deposition for a three-year period from 2006 to 2008 (Kuramoto et al., 2011). The value at NEGIS was the average over 1607–2011 (Vallelonga et al., 2014). A comparison between these deposition results and our data indicated that the rate of accumulation was lower (below 85%) at the EGRIP site than at other sites in recent years, except for NEGIS.

The NEGIS drilling site and our pit sites are very close, separated by 1.7 km (Pit 1) and 1.2 km (Pit 2). Vallelonga et al. (2014) reported that annual layer thicknesses at NEGIS were, on average, 0.11 m ice equivalent (i.e.) in 1607–2011, ranging from 0.08 to 0.14 m i.e. in a firn core study. These values can be converted to 0.10, 0.07 and 0.13 m w.e. assuming an ice density of 917 kg m^{-3}. The authors also concluded that the maximum value of 0.14 m i.e. corresponded to the annual layer thickness in A.D. 1860, when the ice at the drilling site had been located at lower elevations upstream. They suggested that this depression of elevation collected blowing snow, thereby increasing local accumulation and contributing to the thickening of the annual layers. Although NEGIS and our pit sites are very close, the mean deposition values obtained in this study were around 50% higher than the average value given in Vallelonga et al. (2014). It is possible that annual deposition at the EGRIP site increased in recent years. However, we lack sufficient data to provide an explanation beyond what Vallelonga et al. (2014) reported on the interplay between topographic undulations and accumulation effects. Our recent study (Komuro et al., 2020) discussed the spatial and temporal variability in recent annual snow deposition in the EGRIP area, pointing out that post-depositional redistribution of snow by wind erosion and snowdrift was likely in the area. However, we found little variability in average snow deposition over multiple years (ranging from 148 to 157 mm w.e. Yr^{-1}) and in the annual average snow deposition across multiple pits (ranging from 134 to 157 mm w.e. Yr^{-1}). In addition, snow deposition in the area was nearly constant during 2009–2017.

3.4. Seasonality of major ion species and dust

The ion and dust concentration records displayed seasonal variation (Fig. 5). The peaks of both K^+ and NH_4^+ concentrations in the pit profiles tended to appear at the same or similar depths, corresponding to summer layers. In addition, some peaks appeared in the layers between the winter and the following summer. Biomass burning has a strong seasonal cycle, peaking in the summer (e.g., Hu et al., 2013). Historically, a high concentration of K^+ in the snow and ice in Greenland has been attributed mainly to biomass burning at lower latitudes (e.g., Legrand and Mayewski, 1997; Kuramoto et al., 2011). However, because K^+ has other sources, NH_4^+, black carbon, and organic compounds have recently been recognized as more useful indicators of biomass burning (Legrand et al., 2016). Increases in the NH_4^+ concentration have been found in some summer layers of snow and ice deposited in other Greenland regions and have been used as a proxy of biomass burning (e.g., Legrand et al., 1992; Whitlow et al., 1994; Dibb et al., 2007; Zennaro et al., 2014; Legrand et al., 2016). Furthermore, many of these studies use soluble K^+ deposition to detect biomass burning events.

Table 1
Summary of average annual deposition for the present day at other deep ice core drilling sites in Greenland and the EGRIP site.

Site	Position	Elevation	Accumulation in water equivalent	Reference
NEEM	77.45°N 51.06°W	2484 m	20 cm/yr	Steen-Larsen et al. (2011)
NEEM	77.4469°N 50.9464°W		17.6 cm/yr	Kuramoto et al. (2011)
GRIP	72.58°N 38.50°W	3230 m	23 cm/yr	Steen-Larsen et al. (2011)
North GRIP	75.10°N 42.32°W	2919 m	19 cm/yr	Steen-Larsen et al. (2011)
Dye 3	65.18°N 43.83°W	2490 m	50 cm/yr	Steen-Larsen et al. (2011)
Camp Century	77.18°N 61.15°W	1890 m	35 cm/yr	Steen-Larsen et al. (2011)
NEGIS	75.62°N 35.96°W	2700 m	10 cm/yr	Vallelonga et al. (2014)
EGRIP	75.6289°N 36.0039°W	2666 m	13.8 cm/yr	This study
EGRIP	75.6252°N 35.9860°W	2660 m	14.9 cm/yr	This study

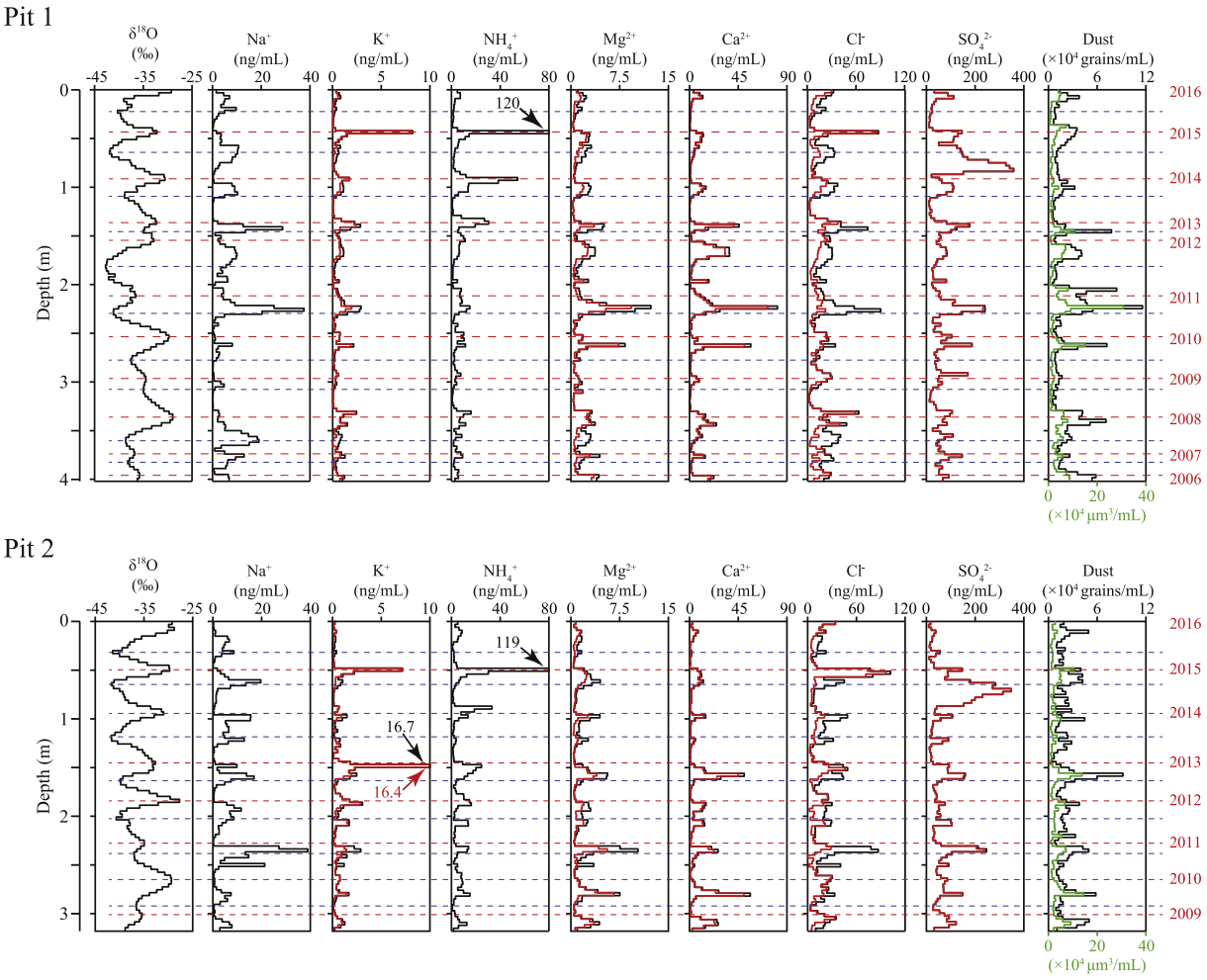

Fig. 5. Vertical profiles of $\delta^{18}O$, ion, and dust concentrations. Black and red curves for five ion species indicate total concentrations of the five ions and non-seasalt (nss) fractions, respectively. Dust is shown in number (black) and in volume (green) concentrations. Red dotted lines indicate annual summer boundaries similar to Fig. 3. Blue dotted lines show annual winter boundaries defined from minimum values of $\delta^{18}O$. (For interpretation of the references to colour in this figure legend, the reader is referred to the Web version of this article.)

The profiles of NH_4^+ in the pits in this study frequently exhibited summer peaks at the same depths where peaks of non-sea-salt components of K^+ ($nssK^+$) were observed (Fig. 5). The $nssK^+$ was calculated with the following equation by considering the mass ratio of potassium to sodium in seawater:

$$[nssK^+] = [K^+] - (K^+/Na^+)_{sea} \times [Na]$$

where $(K+/Na+)_{sea}$ is the mass ratio of K^+/Na^+ in the sea water, which is 0.038. Similarly, concentrations of $nssMg^{2+}$, $nssCa^{2+}$, and $nssSO_4^{2-}$, which are discussed later in this section, were calculated using sea-water ratios of 0.12, 0.0384 and 0.251, respectively (Li et al., 2016). Correlation coefficients for the relationships between concentrations of $nssK^+$ and NH_4^+ were 0.85 ($n = 134$, $p < 0.01$) for Pit 1 and 0.55 ($n = 106$, $p < 0.0001$) for Pit 2. The agreement in the timing of enhanced concentrations of $nssK^+$ and NH_4^+ in summer snow layers suggest that the seasonal variation in those components in snow at the EGRIP site originated from biomass burning.

The sources of $nssK^+$ and NH_4^+ explaining the concentration peaks between winter and next summer layers are unclear. Kuramoto et al. (2011) reported that concentrations of $nssK^+$ show a peak in the winter to spring layers in a snow pit at the NEEM (77°27′N, 50°57′W, 2600 m a.s.l.). However, they did not identify the source of the peaks. This issue is an open question and should be addressed in further studies.

The extremely high summer peak of both the nssK^+ and NH_4^+ concentration in 2015 may arise from an intense biomass burning event in Alaska and Canada between late June and early July 2015, which influenced the European Arctic. This event caused unusually high aerosol optical depths over a vast area of the European Arctic from Ny-Ålesund and Hornsund reaching as far as northern Scandinavia in July (Markowicz et al., 2016). In Svalbard, the value was the highest recorded since 2005. This event seems to have influenced snow at EGRIP as well, resulting in the highest levels of nssK^+ and NH_4^+ since 2006 in our pits.

Seasonal variation in the SO_4^{2-} concentration seemed to be less pronounced in both pits although these peaks appeared relatively frequent between winter and next summer seasons (Fig. 5). Studies in northern, central, and southern Greenland have reported that the concentrations of SO_4^{2-} in snow and ice generally follow a similar seasonal pattern, peaking in winter to spring (Finkel et al., 1986; Beer et al., 1991; Whitlow et al., 1992; Jaffrezo et al., 1994; Fischer et al., 1998; Bigler et al., 2002; Dibb et al., 2007; Kuramoto et al., 2011). The profile of SO_4^{2-} concentrations in this study suggests that the snow pits in northeastern Greenland show the same seasonal trend as those reported in previous studies. Although we could not identify the spring layers, according to these previous studies, the maximum SO_4^{2-} concentrations in our pits may have occurred in winter to spring seasons.

The source of the SO_4^{2-} concentration peaks in the winter to spring layers was likely anthropogenic inputs. Potential sources of SO_4^{2-} in snow and ice of Greenland include dust, volcanic eruptions, sea salt, SO_2 resulting from combustion of fossil fuels, and DMS given off by phytoplankton in the ocean (Legrand et al., 1995; Legrand, 1997; Legrand and Mayewski, 1997). However, dust and DMS contributions in this study are very low because the peaks of dust and MSA from DMS oxidation appeared at different depths from those of the SO_4^{2-} peaks. In addition, potential sources of sea salt are negligible because nssSO_4^{2-} accounts for an average of 98.2 ± 1.9% and 98.0 ± 2.1% of the total sulfate for Pit 1 and Pit 2, respectively. These low contributions suggest that the winter-to-spring peak resulted from the inflow of air pollutants caused by fossil fuel combustion.

Our nssSO_4^{2-} data recorded the signal from the 2014 Bárðarbunga-Veiðivötn fissure eruption at Holuhraun in Iceland. The eruption lasted from August 31, 2014 to February 28, 2015 and was the largest eruption in Iceland in more than 200 years (Schmidt et al., 2015). The signal of this eruption was also found in another snow pit study at the EGRIP in 2017 (Du et al., 2019). Our detailed data at 3-cm intervals showed high nssSO_4^{2-} concentrations from immediately above the 2014 summer layer to immediately above the 2014/15 winter layer, corresponding to the eruption period (Fig. 5). Because the eruption of Bárðarbunga released rich gas (SO_2) and poor ash, the volume of tephra produced during this eruption was not substantial (Galeczka et al., 2016). In addition, the particle concentrations were very low, as determined using an Optical Particle Counter (particle size of 0.3–10 μm) installed 72 km from the main eruption vent, similar to concentrations in dormant conditions. The dust concentrations in the layers of our pit were not high, supporting the low tephra production.

The concentrations of Na^+ and Cl^- were correlated, with correlation coefficients of 0.710 ($p < 0.01$) and 0.593 ($p < 0.05$) for Pit 1 and Pit 2, respectively. The correlation coefficient for this relationship in a snow pit at the NEEM (Kang et al., 2015) was 0.621 ($p < 0.01$), similar to those in our data. However, a pit study at EGRIP by Du et al. (2019) showed a relatively strong correlation ($r = 0.874$, $p < 0.01$). In previous studies in Greenland, concentrations of Na^+ and Cl^- in snow and ice were thought to originate primarily from sea spray aerosols (e.g., Legrand and Mayewski, 1997; Kang et al., 2015; Du et al., 2019). Additional sources of Cl^- are gaseous HCl or chloride compounds from anthropogenic sources in the summer and increase the Cl^-/Na^+ concentration ratio (hereafter termed the "Cl^-/Na^+ ratio") in summer snow at Greenland sites (e.g., Dibb et al., 2007; Kang et al., 2015).

Scatter plots of Cl^- vs. Na^+ concentrations for Pit 1 and Pit 2 (Fig. 6) show two clusters, distinguishing between sea-salt Cl^- and nssCl^- as the main sources. The slopes of the regression lines for samples with low Cl^-/Na^+ ratios were 2.10 and 2.16 for Pit 1 and Pit 2, respectively. These values were close to that of seawater (1.8). In addition, the high coefficient of determination of the regression line ($R^2 = 0.87$ for both pits) indicated that when the Cl^-/Na^+ ratio is low, Cl^- in snow could be regarded as a proxy for sea salt aerosol. Snow samples with Cl^-/Na^+ ratios exceeding 10 seemed to be strongly influenced by additional sources of Cl^-. The R^2 value for the regression line was lower than that of the other cluster. This result indicates that the contribution of sodium-free chloride is dominant. Our pit studies at the EGRIP indicated that Cl^- in snow does not reflect only marine sources, as was reported for the EGRIP snow by Du et al. (2019), but can be attributed to multiple sources, consistent with previous studies of snow chemistry at other Greenland sites. Seasonality and Cl^-/Na^+ ratios will be discussed further in Sections 3.5 and 3.6.

NssMg^{2+} and nssCa^{2+} in the snow at various Greenland sites are commonly used as mineral dust proxies and peak between the winter and spring, according to previous studies (e.g., Dibb et al., 2007; Kuramoto et al., 2011). The concentrations of these ions and dust in snow at EGRIP exhibited similar trends (Fig. 5). The peak concentrations usually appeared in the layers between the winter and the following summer season. There were strong relationships between concentrations of nssMg^{2+} and nssCa^{2+} ($r = 0.910$, $p < 0.01$ and $r = 0.930$, $p < 0.01$ for Pit 1 and Pit 2, respectively). This suggests that nssMg^{2+} and nssCa^{2+} in the snow were derived from the same source. The nssMg^{2+} concentrations

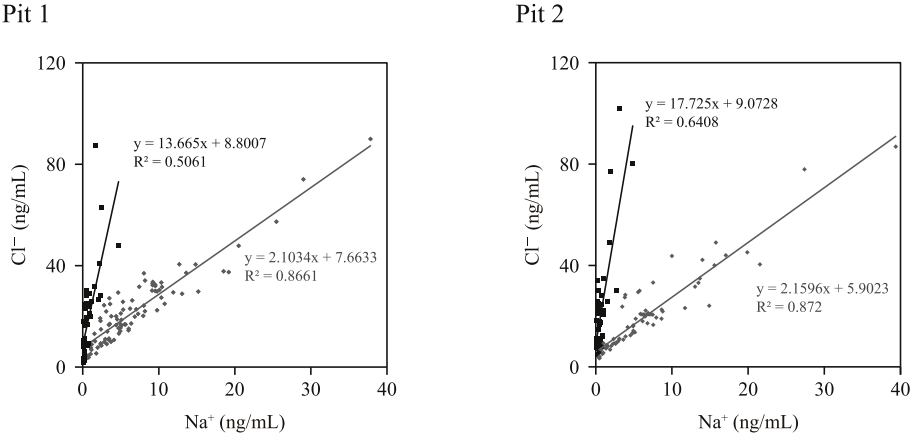

Fig. 6. Scatter plots of Cl− vs. Na + concentrations for Pit 1 and Pit 2. Snow samples with a Cl^-/Na^+ ratio of <10 are shown as gray circles in the figure. Black circles indicate samples with a ratio of >10.

were correlated with the total volume of dust particles ($r = 0.813$ and 0.847) and the total number of dust particles ($r = 0.712$ and 0.761) in the two pits. Concentrations of $nssCa^{2+}$ were also related to the total volume of dust ($r = 0.792$ and 0.880) and total number of dust particles ($r = 0.686$ and 0.807). All correlation coefficients were significant at $p < 0.01$. Thus, $nssMg^{2+}$ and $nssCa^{2+}$ originated mainly from dust. The contributions of $nssMg^{2+}$ to total Mg^{2+} were 0.725 ± 0.202 and 0.726 ± 0.197 for Pit 1 and Pit 2, respectively. Those for $nssCa^{2+}$ were 0.958 ± 0.046 and 0.950 ± 0.062 for Pit 1 and Pit 2.

3.5. Chemical components with annual maxima and minima in the summer

The concentration of NO_3^- and Cl^-/Na^+ ratio peaked in the summer layers, whereas pH values were relatively low (Fig. 7). The same seasonality in pH was also observed in a snow pit study at NEEM (Kuramoto et al., 2011), although seasonal variation in pH was not clear. Similarly, summer NO_3^- peaks were observed in snow pit and ice core studies at other sites on the Greenland ice sheet (e.g., Steffensen, 1988; Beer et al., 1991; Whitlow et al., 1992; Fischer et al., 1998; Motoyama et al., 2001; Dibb et al., 2007; Kuramoto et al., 2011). The summer NO_3^- peak is

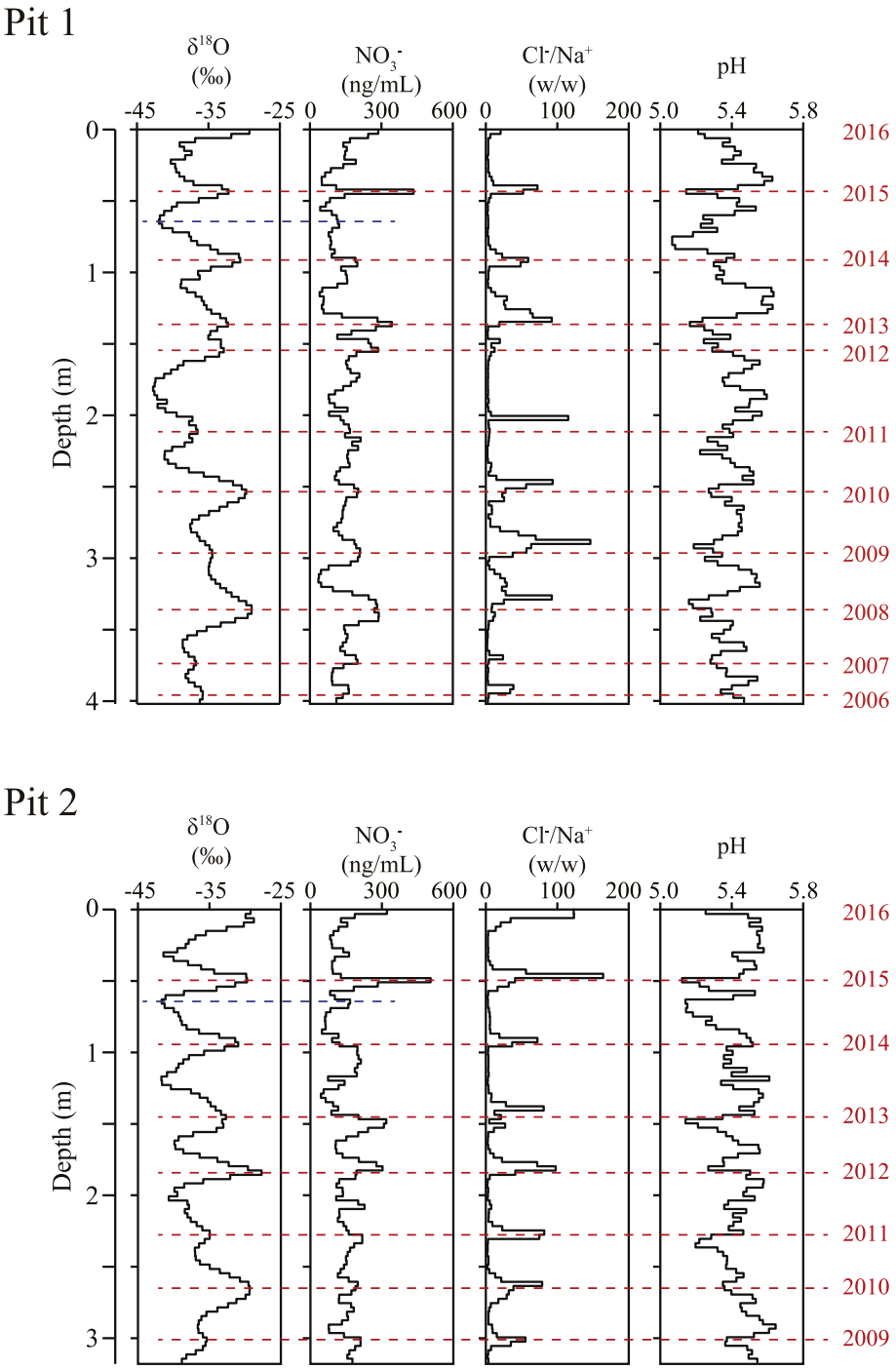

Fig. 7. Vertical profiles of the $\delta^{18}O$ value, NO_3^- concentration, Cl^-/Na^+ concentration ratio, and pH for Pit 1 and Pit 2. Red dotted lines indicate annual boundaries similar to Fig. 2. Each blue dotted line indicates the 2014/2015 winter layer defined from the minimum value of $\delta^{18}O$. (For interpretation of the references to colour in this figure legend, the reader is referred to the Web version of this article.)

thought to be explained by NO_X produced by natural (lightning, soil microbial processes, and stratospheric N_2O oxidation) and anthropogenic (fossil fuel combustion and biomass or biofuel burning) processes (e.g., Fuhrer and Legrand, 1997; Hastings et al., 2004; Fibiger et al., 2013; Zatko et al., 2016).

Estimated NO_3^- loss from surface snow after deposition in the summer ranges from 2% to less than 10% at the summit in Greenland (Burkhart and Hutterli, 2004; Fibiger et al., 2016), unlike estimates for sites with lower rates of accumulation in Antarctica (e.g., Fibiger et al., 2013). Therefore, NO_3^- was largely preserved in the snow and its loss was insignificant at EGRIP.

Some previous studies of the Greenland ice sheet have reported that a winter-to-early spring peak in the NO_3^- concentration can be observed in modern snow at NEEM and Summit (Whitlow et al., 1992; Dibb et al., 2007; Kuramoto et al., 2011) due to anthropogenic NOx from fossil fuel combustion. In this study, high concentrations of NO_3^- were occasionally detected in winter-to-early spring layers.

Our results for the NO_3^- concentration profiles from the two pits did not necessarily correspond to those of another EGRIP pit study by Du et al. (2019). We could not confirm the high concentrations of NO_3^- in the autumn season of 2012. Furthermore, the previous study concluded that a decrease in NO_3^- concentrations in 2014/2015 was caused by the Holuhraun eruption. However, the profiles obtained in the present study indicated relatively high NO_3^- concentrations in the 2014/2015 winter layers of the two pits (Fig. 7), similar to the levels observed by Du et al. (2019). The two pits in our study showed similar concentration profiles of NO_3^-. It is unclear why their results differed from ours. One possible reason is the spatial variability resulting from the post-depositional redistribution of snow caused by wind erosion and snowdrift.

Seasonal variation in the Cl^-/Na^+ ratio is characterized by annual summer peaks in snow at Summit (Whitlow et al., 1992) and the NEEM (Kang et al., 2015; Kuramoto et al., 2011). The summer peaks of the Cl^-/Na^+ ratio every year generally exceeded approximately 1.8 in the mass fraction of seawater (Pytkowicz and Kester, 1971). This enrichment of Cl^- relative to Na^+ is caused by snow/aerosol scavenging of Cl^- derived from gaseous HCl or anthropogenic emissions (Legrand and Delmas, 1988; Kang et al., 2015). Reactions between NaCl in the sea salt particles and acidic species, mainly nitrate, sulfate and organic acids, produce gaseous HCl, while acidic species are enriched in the atmosphere, referred to as dechlorination (Legrand et al., 2002; Li et al., 2016). Thermal and photolytic decomposition of peroxyacetyl nitrate (PAN) is expected to act as a source of NO_2 in the arctic troposphere in the late spring and summer. PAN is a reactive nitrogen species and is the most abundant of the organic reservoir NO_y species ($NO_y = NO_x + HNO_3 + HONO + PAN +$ others) in the Arctic troposphere. PAN accounts for 70%–85% of the measured NO_y (Bottenheim et al., 1993; Muthuramu et al., 1994, Beine and Krognes, 2000). Although NOx has a relatively short lifetime from a few hours to a few days in the troposphere (Tie et al., 2002), PAN shows very long lifetimes of several months in the troposphere (Kirchner et al., 1997, 1999). Therefore, it can be transported over a long distance (Beine and Krognes, 2000). NO_2 is then predominantly lost via its reaction with OH to form HNO_3 (Hastings et al., 2004). Thus, the reaction between sea salt (NaCl) and HNO_3 may be the dominant process for dechlorination in the summer arctic troposphere.

The dominant fraction of oxidized nitrogen (NO_y) transported to Summit in Greenland is PAN (Kramer et al., 2015). Several studies have suggested that PAN accumulation during the arctic winter and subsequent decomposition in the spring and summer contribute to the high NO_3^- concentrations observed in snow during the warmer months (e.g., Munger et al., 1999; Yang et al., 1995). This may explain the contribution of PAN in the Arctic to high NO_3^- concentrations, relatively low pH values, and enrichment of Cl^- concentrations in the summer layers observed in our snow pits in 2016.

Our results for the Cl^-/Na^+ ratio also differed from those of Du et al. (2019), who found a peak in the Cl^-/Na^+ ratio in the summer layer of 2016 at EGRIP. They concluded that a proportion of Cl^- was derived from seawater due to an extremely warm period, substantially reducing the sea ice area in that year. Although only a part of the 2016 summer peak appeared in the profile of the Cl^-/Na^+ ratio for Pit 2 in this study, we think that the 2016 peak was not extraordinary compared with those for other years. In fact, additional Cl^- input is believed to arise from anthropogenic emissions or gaseous HCl, including sea-salt dechlorination. The warming event and reduction of sea ice area emphasized by Du et al. (2019) cannot explain the input of only Cl^- without Na^+ to the atmosphere.

3.6. Cl^-/Na^+ ratio

The annual summer peaks of the Cl^-/Na^+ ratio in our pits at EGRIP were much higher than those reported in previous studies at other sites in Greenland (Whitlow et al., 1992; Kuramoto et al., 2011; Kang et al., 2015; Oyabu et al., 2016). The ratios at EGRIP were 24.24–165.9 and typically exceeded 56 in the summer. In contrast, the Cl^-/Na^+ ratios in summer snow layers were no greater than 50 for Summit (Whitlow et al., 1992) and were below 40 for the NEEM (Kuramoto et al., 2011; Kang et al., 2015). Furthermore, the South East Dome (SE-Dome) showed an average Cl^-/Na^+ of 1.02 over the entire depth of a 3.55 m snow pit, with a high Cl^-/Na^+ ratio of about 4.5 at a depth of 3.55 m (Oyabu et al., 2016). However, because SE-Dome has a high rate of accumulation of 1.01 m w.e. Yr^{-1} according to Iizuka et al. (2018), the pit analyzed by Oyabu et al. (2016) may not have included the summer layer with a high excess-Cl^- concentration.

One explanation for the difference in Cl^-/Na^+ ratios among sites is the distance of aerosol transport. The reaction between sea salt (NaCl) and NO_3^- produced by PAN may generate gaseous HCl, as described in Section 3.5. The fraction of gaseous HCl deposition as well as aerosol particles should differ between coastal and inland regions in Greenland, as indicated by Oyabu et al. (2016). The Arctic is a major receptor for anthropogenic pollution transported from mid-latitudes (Quinn et al., 2007). Similarly, PAN in the Arctic is derived primarily from combustion processes in industrialized areas in mid-latitudes (Beine and Krognes, 2000). Global models have recently shown that a variety of sources from mid-latitude regions contribute to pollutant distributions in the Arctic (Koch and Hansen, 2005; Shindell et al., 2008; Stohl, 2006). Long-distance transportation could provide time for NaCl in the sea salt particles to react with atmospheric acidic species. The air masses are transported toward the Arctic, causing an increase in gaseous HCl-rich air. Therefore, the migration distance and deposition fraction of HCl appear to explain the significant increase in the Cl^-/Na^+ ratio at EGRIP.

3.7. Comparison of results for seasonal changes in EGRIP snow chemistry between studies

The results of the present study differed from those of a previous study at the EGRIP site reported by Du et al. (2019) in several aspects. They investigated the seasonal variations in stable water isotope ($\delta^{18}O$, δD, and d-excess) as well as dust and major ion (Ca^{2+}, Na^+, Cl^-, MSA, SO_4^{2-}, NH_4^+ and NO_3^-) concentrations recorded in a single pit. Below, we discuss the similarities and differences between our results and theirs.

The same seasonal variations of $\delta^{18}O$, δD, and d-excess were observed in both studies. The $\delta^{18}O$ and δD values had maxima in the summer layer and minima in the winter layer. The d-excess value had maxima and minima in the autumn and from spring to early summer, respectively. Du et al. (2016) reported that the lower d-excess values appeared during the winter in 2012 and 2014, corresponding to the depths where $\delta^{18}O$ and δD had minimum values. They considered that the Holuhraun eruption in 2014 and snow melting events in 2012 may have caused the abnormal d-excess values. However, our d-excess data from the two pits did not show such minimum values in the winter, but rather indicated normal seasonal cycles. Moreover, our other pit studies at the EGRIP site (Komuro et al., 2020) also found that the d-excess

values followed normal seasonal cycles in 2012 and 2014. Therefore, we consider that the signals of d-excess associated with the Holuhraun eruption in 2014 and snow melting event in 2012 may not have been recorded in the snow at EGRIP.

The same seasonal variation in Ca^{2+} concentration was observed in both studies. Similarly, the contributions of $nssCa^{2+}$ to total Ca^{2+} were around 95%, and $nssCa^{2+}$ appeared to originate mainly from dust. However, unlike Du et al. (2019), the Ca^{2+} concentration peak of 2014 that they considered to be exceptionally high was not so high in our pits when looking at longer-term records.

The interpretation of Na^+ and Cl^- concentrations by Du et al. (2019) differed from that of this study. As mentioned in Section 3.4, they considered that Na^+ and Cl^- originated from a marine source. However, in the present study, although Na^+ seemed to originate mainly from a marine source, Cl^- in snow reflected no only marine sources but multiple sources. Our results were consistent with previous snow chemistry studies at other Greenland sites.

Du et al. (2019) reported that high MSA concentrations were observed in the 2014 and 2017 summer layers, suggesting that higher temperatures (higher $\delta^{18}O$ and δD) and lower sea ice occurred in both years. The MSA concentration data from the two pits in the present study showed that relatively high concentration appeared in the summers of 2013, 2014, and 2015, which were similar to the concentration levels observed in their study. However, the $\delta^{18}O$ and δD values were not high, but rather normal levels. Therefore, we consider that an argument for the relationship between MSA concentration and extent of sea ice must be made more carefully.

It can be deduced from both studies that the EGRIP snow record shows an $nssSO_4^{2-}$ signal peak reflecting the 2014 Holuhraun eruption. However, the suggestion by Du et al. (2019) that a significant short-term cooling effect occurred during this eruption be cannot supported by the results of the present study. As stated in above, the seasonal variations in stable water isotope observed in the present study and the study by Komuro et al. (2020) indicated normal seasonal cycles during the Holuhraun eruption period. Therefore, opinions are divided on this issue.

The extremely high summer peak of NH_4^+ concentration in 2015 was observed in both pit studies. Although we attributed the peak to a biomass burning event in Alaska and Canada in the summer of 2015, Du et al. (2019) considered it to be associated with gas emissions from the Holuhraun eruption. In both studies, the NH_4^+ concentration did not increase during the eruption period, which was not the case for the $nssSO_4^{2-}$ concentration. Volcanic eruptions inject sulfur into the atmosphere mainly in the form of SO_2 and H_2S gasses, which are subsequently converted to sulfate. Therefore, we considered that the high peak of NH_4^+ concentration was not associated with gas emissions from the Holuhraun eruption. Although their study did not include an $nssK^+$ concentration profile, the $nssK^+$ concentration reported in the present study showed an extremely high peak in the same layer. Therefore, we considered that the $nssK^+$ and NH_4^+ concentration peaks may have arisen from the intense biomass burning event mentioned in Section 3.4. While opinions vary as to the origin of the NH_4^+ concentration peak, the peak has been recorded in the EGRIP snow and can be used as a signal in ice core studies.

The NO_3^- concentration profiles from the two pits in this study did not necessarily correspond to those reported by Du et al. (2019). As described in Section 3.5, the similar NO_3^- concentration profiles were observed in the two pits of this study. However, the profile obtained from their study did not resemble our profiles, except that a relatively high concentration peak was observed in the summer of 2015 in both studies. The reason for the discrepancies in the results remains unclear.

There was no substantial difference in dust concentrations between the two studies. The relatively high concentration layers in 2013 appeared in the profiles of both studies. In addition, the relatively low dust concentrations duing the Holuhraun eruption period were also a common feature.

4. Conclusions

We describe the results of two pit observations conducted at EGRIP in 2016. Pit 1 was 4.02 m deep and included ten years of snow deposition (2006–2016). Pit 2 was 3.18 m deep and covered the period between 2009 and 2016. Average recent annual snow deposition reconstructed by seasonal variation in the pit profiles in $\delta^{18}O$, δD, d-excess and MSA were as follows: 138 mm w.e. in 2006–2016 for Pit 1, 145 mm w.e. in 2009–2016 for Pit 1, and 149 mm w.e. in 2009–2016 for Pit 2. These values were less than 85% of the recent annual snow thicknesses reported at other sites in Greenland and indicated that deposition at the EGRIP site is relatively low. A comparison between NEGIS and our EGRIP pits, located 1.7–1.2 km apart, suggested that annual deposition at the EGRIP site has increased in recent years.

Concentration profiles of K^+, NH_4^+, SO_4^{2-}, Cl^-, Na^+, Mg^{2+}, Ca^{2+}, and dust in our snow pits showed the same seasonality as that observed at other sites on the Greenland ice sheet and had annual maximum peaks between winter and the next summer season. Our pits included signal peaks for the $nssSO_4^{2-}$ concentration from the 2014 Bárðarbunga-Veiðivötn fissure eruption at Holuhraun in Iceland. Additionally, a biomass burning event in Alaska and Canada in the summer of 2015 likely explained the extremely high peaks of $nssK^+$ and NH_4^+ concentrations in the pits. Mg^{2+} and Ca^{2+} concentrations were highly correlated with the total volume of dust particles, suggesting that these ions originated from dust.

NO_3^- concentrations and the Cl^-/Na^+ ratio peaked in the summer, while pH values were relatively low in the summer layers. The summer peaks in the NO_3^- concentration and Cl^-/Na^+ ratio observed at EGRIP were consistent with those in previous snow pit and ice core analyses at other sites on the Greenland ice sheet. The conversion of PAN to HNO_3 and dechlorination in the summer Arctic troposphere appear to play an important role in increases in the NO_3^- concentration and Cl^-/Na^+ ratio and a decrease in the pH value.

The Cl^-/Na^+ ratios for the summer peak in our pits at EGRIP were much higher than those at other sites in Greenland. The differences in transport distance, resulting in an increase in HCl-rich vapors by dechlorination, and deposition fraction of HCl on the snow surface may have led to the large difference in the Cl^-/Na^+ ratio among sites in Greenland.

Finally, we discussed the similarities and differences between the results of the present study and a previous EGRIP pit study by Du et al. (2019). We consider additional work to be needed to resolve areas of disagreement.

Declaration of competing interest

The authors declare that they have no known competing financial interests or personal relationships that could have appeared to influence the work reported in this paper.

Acknowledgements

EGRIP is directed and organized by the Center of Ice and Climate at the Niels Bohr Institute and US NSF, Office of Polar Programs. It is supported by funding agencies and institutions in Denmark (A. P. Møller Foundation, UCPH), US (US NSF, Office of Polar Programs), Germany (AWI), Japan (NIPR and ArCS), Norway (BFS), Switzerland (SNF), France (IPEV, IGE), and China (CAS). We thank the EGRIP field members and the laboratory technicians at NIPR who so generously assisted in conducting this study. This work was supported by the Arctic Challenge for Sustainability (ArCS) Project (Program Grant Number JPMXD1300000000), Japan; and by JSPS KAKENHI Grant Number JP18H04140, Japan; and was partially funded by the Arctic Challenge for Sustainability II (ArCS II) (Program Grant Number JPMXD1420318865), Japan; by the Environment Research and Technology Development Funds (JPMEERF20172003 and

JPMEERF20202003) of the Environmental Restoration and Conservation Agency of Japan, Japan; and by National Institute of Polar Research (Project Research KP305), Japan.

References

Aoki, T., Matoba, S., Uetake, J., Takeuchi, N., Motoyama, H., 2014. Field activities of the "snow impurity and glacial microbe effects on abrupt warming in the arctic"(SIGMA) project in Greenland in 2011-2013. Bull. Glaciol. Res. 32, 3–20.

Beer, J., Finkel, R.C., Bonani, G., Gäggeler, H., Görlach, U., Jacob, P., Klockow, D., Langway Jr., C.C., Neftel, A., Oeschger, H., Schotterer, U., Schwander, J., Siegenthaler, U., Suter, M., Wagenbach, D., Wölfli, W., 1991. Seasonal variations in the concentrations of ^{10}Be, Cl^-, NO_3^-, SO_4^{2-}, H_2O_2, ^{210}Pb, ^{3}H mineral dust and $\delta^{18}O$ in Greenland snow. Atmos. Environ. 25 (5–6), 899–904.

Beine, H.J., Krognes, T., 2000. Seasonal cycle of peroxyacetyl nitrate (PAN) in the European arctic: atmospheric environment. Atmos. Environ. 34 (6), 933–940.

Bigler, M., Wagenbach, D., Fischer, H., Kipfstuhl, J., Miller, H., Sommer, S., Stauffer, B., 2002. Sulphate record from a northeast Greenland ice core over the last 1200 years based on continuous flow analysis. Ann. Glaciol. 35, 250–256. https://doi.org/10.3189/172756402781817158, 2002.

Bottenheim, J.W., Barrie, L., Atlas, A.E., 1993. The partitioning of nitrogen oxides in the lower Arctic troposphere during spring 1988. J. Atmos. Chem. 17, 15–27.

Burkhart, J.F., Hutterli, M., 2004. Seasonal accumulation timing and preservation of nitrate in firn at Summit, Greenland. J. Geophys. Res. 109, D19302. https://doi.org/10.1029/2004JD004658.

Dibb, J.E., Whitlow, S.I., Arsenault, M., 2007. Seasonal variations in the soluble ion content of snow at Summit, Greenland: constraints from three years of daily surface snow samples. Atmos. Environ. 41 (24), 5007–5019.

Du, Z., Xiao, C., Zhang, Q., Li, C., Wang, F., Liu, K., Ma, X., 2019. Climatic and environmental signals recorded in the EGRIP snowpit, Greenland. Environmental Earth Sciences 78, 170. https://doi.org/10.1007/s12665-019-8177-4.

Fahnestock, M.A., Bindschadler, R., Kwok, R., Jezek, K., 1993. Greenland ice sheet surface properties and ice dynamics from ERS-1 SAR imagery. Science 262, 1530–1534. https://doi.org/10.1126/science.262.5139.1530, 1993.

Fahnestock, M.A., Joughin, I., Scambos, T.A., Kwok, R., Karbill, W.B., Gogineni, S., 2001. Ice-stream-related patterns of ice flow in the interior of northeast Greenland. J. Geophys. Res. 106, 34035–34045. https://doi.org/10.1029/2001JD900194.

Fibiger, D.L., Dibb, J.E., Chen, D., Thomas, J.L., Burkhart, J.F., Huey, L.G., Hastings, M. G., 2016. Analysis of nitrate in the snow and atmosphere at summit Greenland: chemistry and transport. J. Geophys. Res. 121, 5010–5030. https://doi.org/10.1002/2015JD024187.

Fibiger, D.L., Hastings, M.G., Dibb, J.E., Huey, L.G., 2013. The preservation of atmospheric nitrate in snow at Summit, Greenland, Geophys. Res. Lett. 40, 3484–3489. https://doi.org/10.1002/grl.50659.

Finkel, R.C., Langway Jr., C.C., Clausen, H.B., 1986. Changes in precipitation chemistry at Dye 3, Greenland. J. Geophys. Res. 91 (D9), 9849–9855.

Fischer, H., Wagenbach, D., Kipfstuhl, J., 1998. Sulfate and nitrate firn concentrations on the Greenland ice sheet: 1. Large-scale geographical deposition changes. J. Geophys. Res. 103 (D17), 21,927–21,934. https://doi.org/10.1029/98JD01885.

Fuhrer, K., Legrand, M.R., 1997. Continental biogenic species in the Greenland Ice Core Project ice core: tracing back the biomass history of the North American continent. J. Geophys. Res. 102 (C12), 26, 735–26,746. https://doi.org/10.1029/97JC01299.

Galeczka, I., Sigurdsson, G., Eiriksdottir, E.S., Oelkers, E.H., Gislason, S.R., 2016. The chemical composition of rivers and snow affected by the 2014/2015 Bárðarbunga eruption, Iceland. J. Volcanol. Geoth. Res. 316, 101–119. https://doi.org/10.1016/j.jvolgeores.2016.02.017.

Hastings, M.G., Steig, E.J., Sigman, D.M., 2004. Seasonal variations in N and O isotopes of nitrate in snow at Summit, Greenland: implications for the study of nitrate in snow and ice cores. J. Geophys. Res. 109 (D20), D20306. https://doi.org/10.1029/2004JD004991.

Hu, Q.-H., Xie, Z.-Q., Wang, X.-M., Kang, H., Zhang, P., 2013. Levoglucosan indicates high levels of biomass burning aerosols over oceans from the Arctic to Antarctic. Sci. Rep. 3, 3119. https://doi.org/10.1038/srep03119.

Iizuka, Y., Uemura, R., Fujita, K., Hattori, S., Seki, O., Miyamoto, C., Suzuki, T., Yoshida, N., Motoyama, H., Matoba, S., 2018. A 60 year record of atmospheric aerosol depositions preserved in a highaccumulation dome ice core, Southeast Greenland. J. Geophys. Res.: Atmosphere 123, 574–589. https://doi.org/10.1002/2017JD026733.

Jaffrezo, J.L., Davidson, C.I., Legrand, M., Dibb, J.E., 1994. Sulfate and MSA in the air and snow on the Greenland ice sheet. J. Geophys. Res. 99 (D1), 1241–1253.

Johnsen, S.J., Dansgaard, W., White, J.W.C., 1989. The origin of Arctic precipitation under present and glacial conditions. Tellus B 41 (4), 452–468.

Joughin, I., Fahnestock, M., MacAyeal, D., Bamber, J.L., Gogineni, P., 2001. Observation and analysis of ice flow in the largest Greenland ice stream. J. Geophys. Res. 106, 34021–34034. https://doi.org/10.1029/2001jd900087.

Kang, J.H., Hwang, H., Hong, S.B., Hur, S.D., Choi, S.D., Lee, J., Hong, S., 2015. Mineral dust and major ion concentrations in snowpit samples from the NEEM site, Greenland. Atmos. Environ. 120, 137–143. https://doi.org/10.1016/j.atmosenv.2015.08.062.

Komuro, Y., Nakazawa, F., Hirabayashi, M., Goto-Azuma, K., Nagatsuka, N., Shigeyama, W., Matoba, S., Homma, T., Steffensen, J.P., Dahl-Jensen, D., 2020. Temporal and spatial variability of snow deposition at EGRIP, Greenland. Pol. Sci. https://doi.org/10.1016/j.polar.2020.100568 (in press).

Kramer, L.J., Helmig, D., Burkhart, J.F., Stohl, A., Oltmans, S., Honrath, R.E., 2015. Seasonal variability of atmospheric nitrogen oxides and non-methane hydrocarbons at the GEOSummit station, Greenland. Atmos. Chem. Phys. 15, 6827–6849. https://doi.org/10.5194/acp-15-6827-2015.

Kirchner, F., Thuner, L.P., Barnes, I., Becker, K.H., Donner, B., Zabel, F., 1997. Thermal lifetimes of peroxynitrates occurring in the atmospheric degradation of oxygenated fuel additives. Environ. Sci. Technol. 31, 1801–1804.

Kirchner, F., Mayer-Figge, A., Zabel, F., Becker, K.H., 1999. Thermal stability of peroxynitrates. Int. J. Chem. Kinet. 31, 127–144.

Koch, D., Hansen, J., 2005. Distant origins of arctic black carbon: a goddard Institute for space studies ModelE experiment. J. Geophys. Res. 110, D04204. https://doi.org/10.1029/2004JD005296.

Kuramoto, T., Goto-Azuma, K., Hirabayashi, M., Miyake, T., Motoyama, H., Dahl-Jensen, D., Steffensen, J.P., 2011. Seasonal variations of snow chemistry at NEEM, Greenland. Ann. Glaciol. 52 (58), 93–200. https://doi.org/10.3189/172756411797252365.

Legrand, M., 1997. Ice-core records of atmospheric sulfur. Philos. Trans. R. Soc. London, Ser. A B 352, 241–250.

Legrand, M., De Angelis, M., Staffelbach, T., Neftel, A., Stauffer, B., 1992. Large perturbation of ammonium and organic-acids content in the Summit-Greenland ice core: fingerprint from forest fires. Geophys. Res. Lett. 19, 473–475.

Legrand, M., De Angelis, M., Cachier, H., Gaudichet, A., 1995. Boreal biomass burning over the last 80 years recorded in a Summit-Greenland ice core. In: Delmas, R.J. (Ed.), Ice Core Studies of Global Biogeochemical Cycles. NATO ASI Series. Springer-Verlag, Berlin Heidelberg, pp. 347–360.

Legrand, M.R., Delmas, R.J., 1988. Formation of HCl in the antarctic atmosphere. J. Geophys. Res. 93, 7153e7168. https://doi.org/10.1029/JD093iD06p07153.

Legrand, M., Mayewski, P., 1997. Glaciochemistry of Polar ice cores: a review. Rev. Geophys. 35, 219–243. https://doi.org/10.1029/96RG03527.

Legrand, M., McConnell, J., Fischer, H., Wolff, E.W., Preunkert, S., Arienzo, M., Chellman, N., Leuenberger, D., Maselli, O., Place, P., Sigl, M., Schüpbach, S., Flannigan, M., 2016. Boreal fire records in Northern Hemisphere ice cores: a review. Clim. Past 12, 2033–2059. https://doi.org/10.5194/cp-12-2033-2016.

Legrand, M., Preunkert, S., Wagenbach, D., Fischer, H., 2002. Seasonally resolved Alpine and Greenland ice core records of anthropogenic HCl emissions over the 20th century. J. Geophys. Res. 107 (D12), 4139. https://doi.org/10.1029/2001jd001165.

Li, S.-M., Barrie, L.A., Talbot, R.W., Hariss, R.C., Davidson, C.I., Jaffrezo, J.L., 1993. Seasonal and geographic variations of methanesulfonic acid in the Arctic troposphere. Atmos. Environ. 27A (17–18), 3011–3024.

Li, T.-C., Yuan, C.-S., Hung, C.-H., Lin, H.-Y., Huang, H.-C., Lee, C.-L., 2016. Chemical characteristics of marine fine aerosols over sea and at offshore islands during three cruise sampling campaigns in the taiwan strait– sea salts and anthropogenic particles. Atmos. Chem. Phys. Discuss. https://doi.org/10.5194/acp-2016-384.

Markowicz, K.M., Pakszys, P., Ritter, C., Zielinski, T., Udisti, R., Cappelletti, D., Mazzola, M., Shiobara, M., Zawadzka, O., Lisok, J., Petelski, T., Makuch, P., Karasiński, G., 2016. Impact of North American intense fires on aerosol optical properties measured over the European Arctic in July 2015. J. Geophys. Res. 121 (14), 487–14512. https://doi.org/10.1051/epjconf/201817606008.

Motoyama, H., Watanabe, O., Kamiyama, K., Igarashi, M., Goto-Azuma, K., Fujii, Y., Iizuka, Y., Matoba, S., Narita, H., Kameda, T., 2001. Regional characteristics of chemical constituents in surface snow, Arctic cryosphere. Polar Meteorol. Glaciol. 15, 55–66.

Munger, J.W., Jacob, D.J., Fan, S.-M., Colman, A.S., Dibb, J.E., 1999. Concentrations and snow-atmosphere fluxes of reactive nitrogen at Summit, Greenland. J. Geophys. Res. 104, 13,721–13,734.

Muthuramu, K., Shepson, P.B., Bottenheim, J.W., Jobson, B.T., Niki, H., Anlauf, K.G., 1994. Relationships between organic nitrates and surface ozone destruction during Polar Sunrise Experiment 1992. J. Geophys. Res. 99, 25369–25378.

Nghiem, S.V., Hall, D.K., Mote, T.L., Tedesco, M., Albert, M.R., Keegan, K., Shuman, C.A., DiGirolamo, N.E., Neumann, G., 2012. The extreme melt across the Greenland ice sheet in 2012. Geophys. Res. Lett. 39, L20502 https://doi.org/10.1029/2012GL053611, 2012.

Oyabu, I., Matoba, S., Yamasaki, T., Kadota, M.Y., Iizuka, Y., 2016. Seasonal variations in the major chemical species of snow at the South East Dome in Greenland. Pol. Sci. 10, 36–42. https://doi.org/10.1016/j.polar.2016.01.003.

Pytkowicz, R.M., Kester, D.R., 1971. The physical chemistry of seawater. Oceanogr. Mar. Biol. Annu. Rev. 9, 11–60.

Quinn, P.K., Shaw, G., Andrews, E., Dutton, E.G., Ruoho-Airola, T., Gong, S.L., 2007. Arctic haze: current trends and knowledge gaps. Tellus B 59, 99–114.

Schmidt, A., Leadbetter, S., Theys, N., Carboni, E., Witham, C.S., Stevenson, J.A., Birch, C.E., Thordarson, T., Turnock, S., Barsotti, S., Delaney, L., Feng, W., Grainger, R.G., Hort, M.C., Höskuldsson, Á., Ialongo, I., Ilyinskaya, E., Jóhannsson, T., Kenny, P., Mather, T.A., Richards, N.A.D., Shepherd, J., 2015. Satellite detection, long-range transport, and air quality impacts of volcanic sulfur dioxide from the 2014–2015 flood lava eruption at Bárðarbunga (Iceland). J. Geophys. Res. Atmos. 120, 9739–9757. https://doi.org/10.1002/2015JD023638.

Shindell, D.T., Chin, M., Dentener, F., Doherty, R.M., Faluvegi, G., Fiore, A.M., Hess, P., Koch, D.M., MacKenzie, I.A., Sanderson, M.G., Schultz, M.G., Schulz, M., Stevenson, D.S., Teich, H., Textor, C., Wild, O., Bergmann, D.J., Bey, I., Bian, H., Cuvelier, C., Duncan, B.N., Folberth, G., Horowitz, L.W., Jonson, J., Kaminski, J.W., Marmer, E., Park, R., Pringle, K.J., Schroeder, S., Szopa, S., Takemura, T., Zeng, G., Keating, T.J., Zuber, A., 2008. A multi-model assessment of pollution transport to the Arctic. Atmos. Chem. Phys. 8, 5353–5372.

Steen-Larsen, H.C., Masson-Delmotte, V., Sjolte, J., Johnsen, S.J., Vinther, B.M., Bréon, F.-M., Clausen, H.B., Dahl-Jensen, D., Falourd, S., Fettweis, X., Gallée, H., Jouzel, J., Kageyama, M., Lerche, H., Minster, B., Picard, G., Punge, H.J., Risi, C.,

Salas, D., Schwander, J., Steffen, K., Sveinbjörnsdóttir, A.E., Svensson, A., White, J., 2011. Understanding the climatic signal in the water stable isotope records from the NEEM shallow firn/ice cores in northwest Greenland. J. Geophys. Res. 116, D06108. https://doi.org/10.1029/2010JD014311.

Steffensen, J.P., 1985. Microparticles in snow from the South Greenland ice sheet. Tellus 37B (4–5), 286–295.

Steffensen, J.P., 1988. Analysis of the seasonal variation in dust, Cl^-, NO_3^- and SO_4^{2-} in two central Greenland firn cores. Ann. Glaciol. 10, 171–177.

Stohl, A., 2006. Characteristics of atmospheric transport into the Arctic troposphere. J. Geophys. Res. 111, D11306 https://doi.org/10.1029/2005JD006888.

Tedesco, M., Fettweis, X., Mote, T., Wahr, J., Alexander, P., Box, J.E., Wouters, B., 2013. Evidence and analysis of 2012 Greenland records from spaceborne observations, a regional climate model and reanalysis data. Cryosphere 7, 615–630. https://doi.org/10.5194/tc-7-615-2013, 2013.

Tie, X., Zhang, R., Brasseur, G., Lei, W., 2002. Global NO_x production by lightning. J. Atmos. Chem. 43, 61–74.

Trusel, L.D., Das, S.B., Osman, M.B., Evans, M.J., Smith, B.E., Fettweis, X., McConnell, J. R., Noël, B.P.Y., van den Broeke, M.R., 2018. Nonlinear rise in Greenland runoff in response to post-industrial Arctic warming. Nature 564, 104–108. https://doi.org/10.1038/s41586-018-0752-4.

Uemura, R., 2007. Studies on the reconstruction of past temperature changes from stable isotopes of water: records of millennialscale climate change from polar ice cores. Quat. Res. (Japan) 46 (2), 147–164 ([In Japanese with English summary.]).

Uemura, R., Yoshida, N., Kurita, N., Nakawo, M., Watanabe, O., 2004. An observation-based method for reconstructing ocean surface changes using a 340,000-year deuterium excess record from the Dome Fuji ice core. Antarctica. Geophys. Res. Lett. 31 (13), L13216 https://doi.org/10.1029/2004GL019954.

Vallelonga, P., Christianson, K., Alley, R.B., Anandakrishnan, S., Christian, J.E.M., Dahl-Jensen, D., Gkinis, V., Holme, C., Jacobel, R.W., Karlsson, N.B., Keisling, B.A., Kipfstuhl, S., Kjær, H.A., Kristensen, M.E.L., Muto, A., Peters, L.E., Popp, T., Riverman, K.L., Svensson, A.M., Tibuleac, C., Vinther, B.M., Weng, Y., Winstrup, M., 2014. Initial results from geophysical surveys and shallow coring of the Northeast Greenland Ice Stream (NEGIS). Cryosphere Discuss. 8, 1275–1287. https://doi.org/10.5194/tc-8-1275-2014.

Van den Broeke, M., Bamber, J., Ettema, J., Rignot, E., Schrama, E., van de Berg, W.J., van Meijgaard, E., Velicogna, I., Wouters, B., 2009. Partitioning recent Greenland mass loss. Science 326, 984–986. https://doi.org/10.1126/science.1178176.

Wendl, I.A., Eichler, A., Isaksson, E., Martma, T., Schwikowski, M., 2015. 800-year ice-core record of nitrogen deposition in Svalbard linked to ocean productivity and biogenic emissions. Atmos. Chem. Phys. 15, 7287–7300. https://doi.org/10.5194/acp-15-7287-2015.

Whitlow, S., Mayewski, P.A., Dibb, J.E., 1992. A comparison of major chemical species seasonal concentration and accumulation at the South Pole and Summit, Greenland. Atmos. Environ. 26A (11), 2045–2054.

Whitlow, S., Mayewski, P., Dibb, J., Holdsworth, G., Twickler, M., 1994. An ice-core-based record of biomass burning in the arctic and sub-arctic, 1750–1980. Tellus B 46, 234–242.

Yang, Q., Mayewski, P.A., Whitlow, S., Twickler, M., Morrison, M., Talbot, R., Dibb, J.E., Linder, E., 1995. Global perspective of nitrate flux in ice cores. J. Geophys. Res. 100 (D3), 5113–5121.

Zatko, M., Geng, L., Alexander, B., Sofen, E., Klein, K., 2016. The impact of snow nitrate photolysis on boundary layer chemistry and the recycling and redistribution of reactive nitrogen across Antarctica and Greenland in a global chemical transport model. Atmos. Chem. Phys. 16, 2819–2842. https://doi.org/10.5194/acp-16-2819-2016.

Zennaro, P., Kehrwald, N., McConnell, J.R., Schüpbach, S., Maselli, O.J., Marlon, J., Vallelonga, P., Leuenberger, D., Zangrando, R., Spolaor, A., Borrotti, M., Barbaro, E., Gambaro, A., Barbante, C., 2014. Fire in ice: two millennia of boreal forest fire history from the Greenland NEEM ice core. Clim. Past 10. https://doi.org/10.5194/cp-10-1905-2014, 1905–1924.